

Chapter 6

Observation of Fluid–Fluid Immiscibility in Ternary Mixtures of DPPC, DOPC and Cholesterol

6.1 Introduction

As discussed chapter 1, cholesterol–rich domains in biomembranes, called rafts, are believed to be involved in many cellular functions [1, 2, 3, 4, 5]. Biochemical studies on the insoluble membrane fraction obtained from detergent extraction of plasma membranes show that it mainly consists of saturated lipids, such as sphingomyelin and cholesterol. The detergent insoluble fraction, known as detergent resistance membranes (DRM), are believed to come from the rafts [6, 7, 8]. Therefore, ternary mixtures of a saturated lipid, an unsaturated lipid and cholesterol have become a popular model system to study the formation and structure of cholesterol–rich domains. We shall refer to these mixtures as ternary raft mixtures. To date, there is no direct evidence for the existence of rafts in plasma membranes. However, in model membranes of raft forming composition, two fluid phases have been found to coexist, one of them rich in the saturated lipid and other rich in the unsaturated one. These two fluid phases are known as the liquid ordered (l_o) phase and liquid disordered (l_d) phase, respectively, in the literature. Although microscopy and spectroscopy studies show the phase separation, there has been no report of such phase coexistence using diffraction techniques. This discrepancy has been very puzzling and there have been suggestions that the in-plane separation of the two phases may not lead to a macroscopic phase separation [9]. We have carried out x-ray

diffraction studies on oriented multilayers of the ternary raft mixtures in an attempt to detect phase separation and determine the nature of the coexisting phases.

This chapter describes the phase behaviour of ternary mixtures composed of equimolar ratio of dipalmitoyl phosphatidylcholine (DPPC) and dioleoyl phosphatidylcholine (DOPC) at various cholesterol concentrations. We have also studied an equimolar mixture of sphingomyelin, DOPC and cholesterol. Earlier literature relevant to the present study is summarized in section 6.2. Our experimental results on these mixtures are presented in section 6.3. These results provide the first direct evidence of phase separation between two fluid phases in ternary raft mixtures using diffraction techniques. We have constructed the electron density profiles of these phases from our diffraction data in order to understand the effect of cholesterol on these membranes and estimate the composition of the two coexisting phases.

6.2 Earlier studies

Studies on lipid membranes reconstituted with cholesterol have drawn a lot of attention due to their biological significance [10]. The evidence we have so far in support of the existence of rafts is mainly from studies on DRM. However, a recent study on model membranes by Heerkoltz showed that Triton X-100 (a non-ionic surfactant), which is used for detergent extraction, may itself promote domain formation [11]. Therefore, detergent extraction cannot conclusively confirm the presence of pre-existing domains in the membranes.

In order to understand the formation, organization and structure of cholesterol-rich domains, ternary mixtures of saturated lipids (such as DPPC and Sphingomyelin), unsaturated lipids (such as DOPC and POPC) and cholesterol have been extensively investigated using a variety of experimental techniques [9, 12, 13, 14, 15, 16, 17, 18, 19, 20, 21, 22, 23, 24]. Studies on giant unilamellar vesicles (GUVs) and solid supported membranes have found domains of the liquid ordered (l_o) phase, rich in the saturated lipid, coexisting with the liquid disordered (l_d) phase, rich in the unsaturated lipid. The ability of fluorescent dyes to partition differently into the two coexisting fluid phases has been used to visualize phase separation in GUVs [12, 13, 20]. Two-photon fluorescence imaging of GUVs also show shape changes

and budding due to $l_o - l_d$ phase separation [20].

Partial phase diagrams of ternary raft mixtures have been constructed using fluorescence microscopy [13], fluorescence spectroscopy techniques, such as fluorescence resonance energy transfer (FRET), fluorescence anisotropy, lifetime and quenching [15], and fluorescence correlation spectroscopy (FCS)[16, 25]. All these studies surmise the coexistence of the l_o and l_d phases at cholesterol concentrations from ~ 10 to ~ 33 mol% below the chain melting transition temperature (T_m) of the saturated lipid. FCS was used to further characterize the l_o and l_d phases. The value of the average diffusion coefficient of the fluorescence dye DiI-C₁₈ in raft mixtures is about 2.5×10^{-8} cm²/s, whereas its values in the fluid phase of pure DOPC and in the gel domains of DPPC/DOPC mixtures are 6.2×10^{-8} cm²/s and 0.44×10^{-8} cm²/s, respectively. The intermediate value of the diffusion coefficient indicates that lipid mobility in the l_o phase is not as high as in the l_d phase [16, 25]. Electron spin resonance (ESR) has also been used to characterize the l_o phase of DRM obtained from RBL-2H3 cells [23]. The order parameter (~ 0.2) and rotational diffusion rate ($\sim 3 \times 10^8$ s⁻¹) of molecules in the DRM are found to be comparable to those obtained from the raft mixtures. In comparison to the l_d phase, in the l_o phase the bilayers are thicker, lateral diffusion is slower and the bending rigidity is higher [9, 16, 20]. It should be noted here that the symbols l_o and l_d have been used in different contexts in the literature. The two fluid phases observed in binary lipid-cholesterol mixtures in spectroscopy studies have been called l_o and l_d . These two phases have to be cholesterol-rich and cholesterol-poor, respectively. The two fluid phases coexisting in ternary raft mixtures are also often called cholesterol-rich l_o and cholesterol-poor l_d phases in the literature. However, there is some controversy concerning the cholesterol contents of these two phases. Composition and cholesterol content of these fluid phases have been determined recently using nuclear magnetic resonance (NMR) by Veatch et al. [13]. Surprisingly cholesterol contents of both these fluid phases are found to be similar. On the other hand, the fact that the addition of cholesterol converts the gel-fluid coexistence seen in binary mixtures into a fluid-fluid coexistence, suggests that one of the phases is rich in the lipid with saturated chains and the other in the unsaturated one. Therefore, we shall use

the symbols l_o and l_d to denote the lipid phase rich in the saturated lipid and that rich in the unsaturated one, respectively, without making any a priori assumption about their cholesterol contents.

As discussed in chapter 3, $l_o - l_d$ phase coexistence has been proposed even in the case of binary mixtures of cholesterol with lipids with saturated chains [26]. Monolayer studies on phospholipid–cholesterol mixtures also suggest liquid–liquid immiscibility for intermediate cholesterol concentrations, and the formation of a condensed complex at a specific stoichiometric ratio of lipid–cholesterol mixtures [18, 19]. However, diffraction studies on these binary and ternary systems do not show any evidence for fluid–fluid coexistence [9, 27, 28]. X-ray diffraction studies on the ternary raft mixtures give a single lamellar spacing, indicating the presence of a single fluid phase [9].

6.3 Experimental results

A systematic x-ray diffraction study on aligned multilayers of an equimolar mixture of DPPC and DOPC at various cholesterol concentrations (X_c) was carried out at $98 \pm 2\%$ relative humidity (RH). Ternary mixtures with X_c of 0, 2.5, 5, 10, 15, 20, 25, 33, 35 and 40 mol% were studied. Phases were identified from the observed characteristic diffraction patterns. For example, diffraction pattern of the fluid phase consists of 3 to 4 lamellar reflections with the diffuse wide angle reflection too weak to be detected. The gel phase can easily be identified from the two sharp wide angle reflections from the hydrocarbon chains. Phase separation was directly detected from the non overlapping diffraction spots from the individual phases.

Equimolar mixture of DPPC and DOPC show a single fluid (L_α) phase above 35°C . Below 35°C , we have observed two sets of lamellar reflections in the small angle region of the diffraction pattern, indicating coexistence of two phases (Fig. 6.1 a). One of them was identified as the gel ($L_{\beta'}$) phase from its characteristic wide angle reflections, as discussed above. The other phase can be identified as the fluid (L_α) phase since no wide angle reflections were observed in this phase. Addition of DOPC into DPPC bilayers (1:1 molar ratio) completely abolishes the main transition of DPPC and hence the ripple ($P_{\beta'}$) phase is absent.

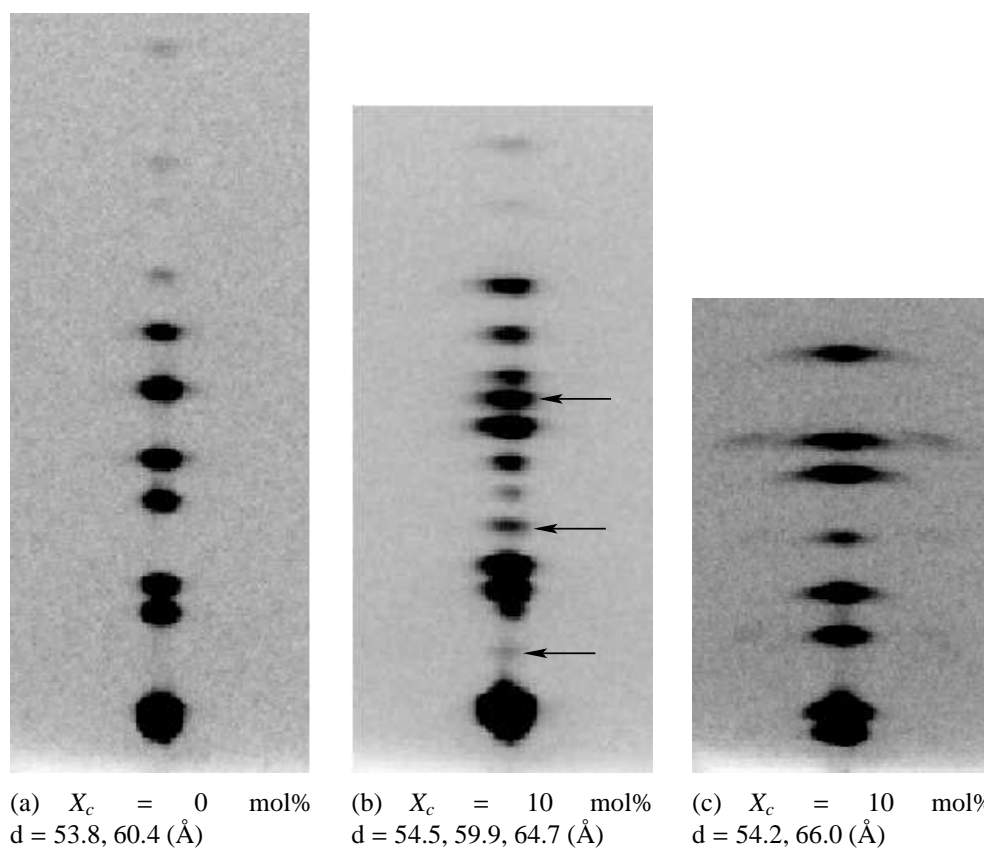


Figure 6.1: Small angle region of the diffraction patterns from an equimolar mixture of DPPC and DOPC at $X_c = 0$ and 10 mol%. The fluid (L_α) phase coexists with the gel ($T = 10^\circ\text{C}$)(a), with the gel and P_β ($T = 24^\circ\text{C}$)(b) and with the P_β phase ($T = 10^\circ\text{C}$) (c). Wavelength of modulation in (c) is ~ 70 Å. Three additional reflections (indicated by arrows) of d-spacing 40.3, 24.4 and 17.5 Å in (b) do not fit into any of the lamellar structures. These reflections always reappear in the same temperature range in successive runs of the sample. At present we do not know the origin of these reflections.

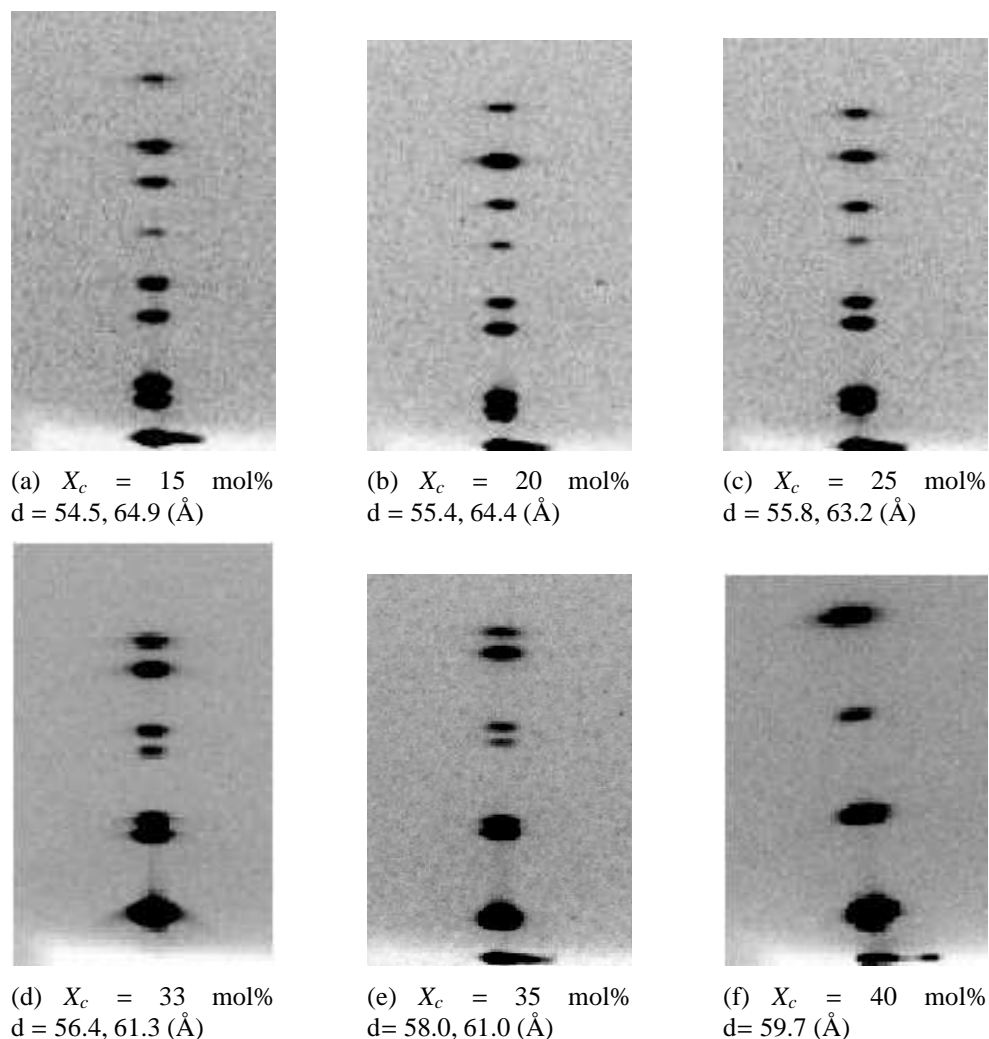


Figure 6.2: Small angle region of the diffraction patterns from an equimolar mixture of DPPC and DOPC as a function of X_c at $T = 10^\circ\text{C}$. The two sets of d-spacings correspond to the coexistence of the l_d and l_o phases.

At $2.5 \leq X_c \leq 10$, the L_α phase is observed above 33°C in the ternary mixtures. It was found to coexist with $L_{\beta'}$ phase from 33°C to 25°C . We have observed a three phase region of L_α , $L_{\beta'}$ and P_β phases from 25°C to 15°C (Fig. 6.1 b). The P_β phase was identified from the satellite reflections seen at lower temperatures and its larger d-spacing compared to that of the $L_{\beta'}$ phase. The P_β phase is a modulated phase induced by cholesterol, as discussed in chapter 3. Below 15°C , L_α phase was found to coexist with P_β (Fig. 6.1 c) and there was no gel phase detected down to the lowest temperature (5°C) studied. At $15 \leq X_c \leq 35$, the coexistence of two fluid phases is found below 30°C (Fig. 6.2). Diffraction pattern at 35°C shows a single fluid phase (Fig. 6.3 a). Wide angle reflections were not seen in the diffraction

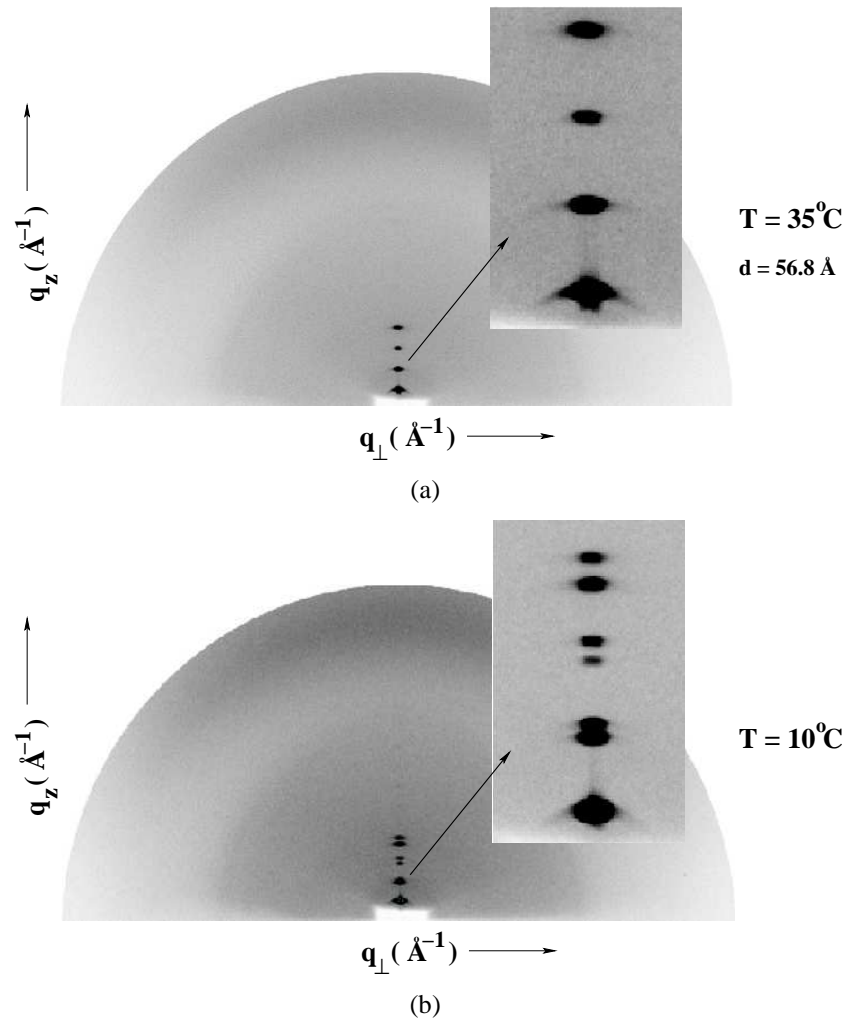


Figure 6.3: Diffraction patterns from an equimolar mixture of DPPC, DOPC and cholesterol showing a fluid phase at 35°C (a) and the coexistence of the two fluid phases at 10°C (b).

Table 6.1: The spacing d (Å) obtained from x-ray diffraction from an equimolar mixture of DPPC and DOPC at various X_c as a function of temperature. Relative humidity was kept fixed at $98 \pm 2\%$. Error in d -spacing is ± 0.2 Å.

T (°C)	X_c (mol%)								
	0	5	10	15	20	25	33	35	40
50	53.9	53.8	54.2	55.3	57.2	56.2	56.0	57.0	59.3
45	53.6	54.4	54.9	55.4	57.2	57.2	56.6	57.2	59.9
40	53.6	54.7	55.3	55.6	57.6	57.0	56.8	57.6	58.6
35	53.6	55.0	55.3	56.0	57.8	57.2	56.8	57.8	58.2
30	53.4 ; 61.3	54.5 ; 57.0	55.0 ; 63.2	55.3 ; 62.4	55.8 ; 61.2	55.3 ; 60.6	56.9	57.8	58.0
25	54.2 ; 61.3	55.4 ; 66.5	54.3 ; 59.9 ; 64.7	56.0 ; 65.2	56.0 ; 63.7	55.3 ; 60.6	58.8	58.8	59.3
20	54.2 ; 61.3	55.4 ; 64.0	54.5 ; 62.2 ; 65.0	55.4 ; 65.5	56.0 ; 64.4	56.2 ; 63.2	56.9 ; 61.3	59.7	59.7
15	53.8 ; 60.6	55.0 ; 64.0	54.5 ; 65.7	54.5 ; 64.9	55.4 ; 64.4	55.8 ; 63.2	56.2 ; 61.3	59.7	59.7
10	53.8 ; 60.4	55.0 ; 63.9	54.2 ; 66.0	54.5 ; 64.9	55.4 ; 64.4	55.8 ; 63.2	56.4 ; 61.3	58.0 ; 61.0	59.7
5	53.4 ; 59.9	54.7 ; 63.8	54.2 ; 66.0	54.5 ; 64.9	55.3 ; 63.9	55.8 ; 63.2	56.4 ; 61.3	57.6 ; 61.0	59.7

pattern from these phases in our experimental geometry (Fig. 6.3 a and b). The d -spacing of one of the fluid phases was found to be similar to that of the L_α phase in binary mixtures of cholesterol with DPPC at similar X_c . This fluid phase, which has a higher d -spacing, was identified as the l_o phase and the other as the DOPC-rich l_d phase. The temperature at which the coexistence of the l_o and l_d phases appears on cooling decreases from 33 to 10°C as X_c is increased from 15 to 35 mol%. At $X_c > 35$ mol%, A single fluid was found to exist down to 5° (Fig. 6.2 f). A pseudo binary phase diagram derived from the diffraction data is shown in Fig. 6.4. The d -spacings obtained from the diffraction data are summarized in table 6.1. Variation of the lamellar d -spacing of the l_o and l_d phases as a function of X_c and temperature are shown in Figs. 6.5 and 6.6, respectively.

We have also studied an oriented sample of an equimolar mixture of sphingomyelin, DOPC and cholesterol in order to check whether it behaves similar to the ternary equimolar mixture described above. This mixture shows a single fluid phase from 50°C to 20°C. Below 20°C, we have observed two sets of reflections, indicating the coexistence of two phases (Fig. 6.7). Wide angle reflections were not seen from either of them, suggesting that they are both fluid phases. These can be identified as the l_o and l_d phases discussed above. The d -spacings of these two fluid phases were found to be 61 Å and 57 Å. In the diffraction pattern (Fig. 6.7), we have observed two additional reflections of d -spacing 39.5 and 24.0 Å. At present we do not have any explanation of the origin of these peaks.

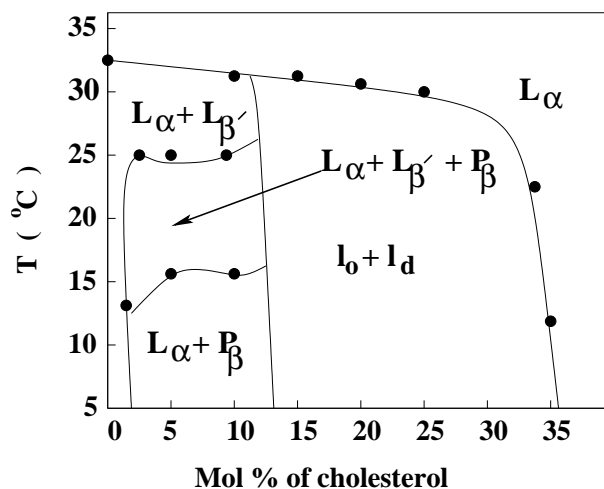


Figure 6.4: Pseudo binary phase diagram of an equimolar mixture of DPPC and DOPC at different X_c , derived from the x-ray diffraction data. L_α : fluid phase, $L_{\beta'}$: gel phase, P_β : modulated phase induced by cholesterol, l_o : fluid phase rich in DPPC, l_d : fluid phase rich in DOPC.

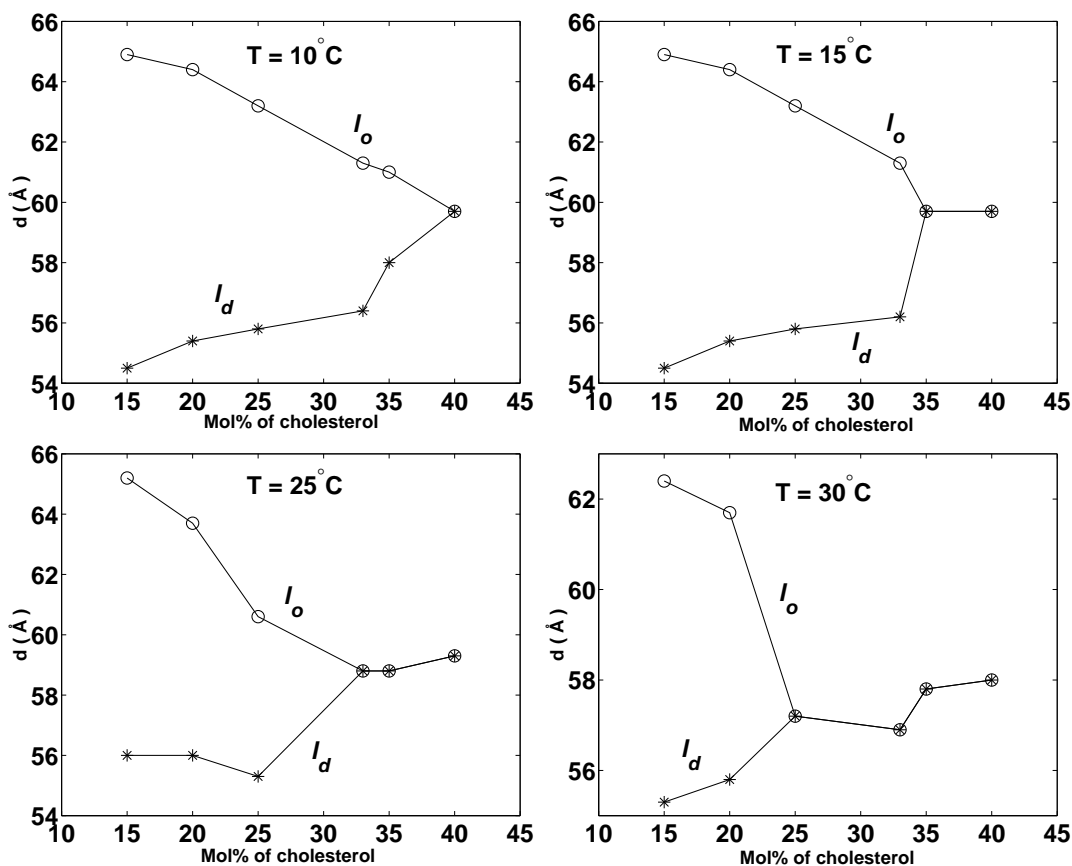


Figure 6.5: Variation of d-spacing of the l_o and l_d phases with X_c at different temperatures.

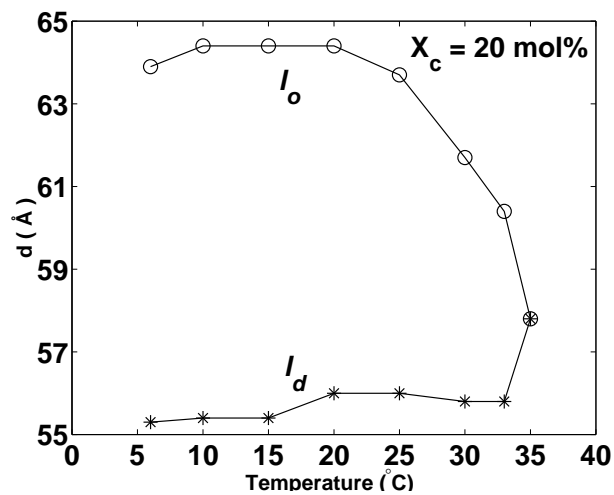


Figure 6.6: Variation of d-spacing of the l_o and l_d phases with temperature.

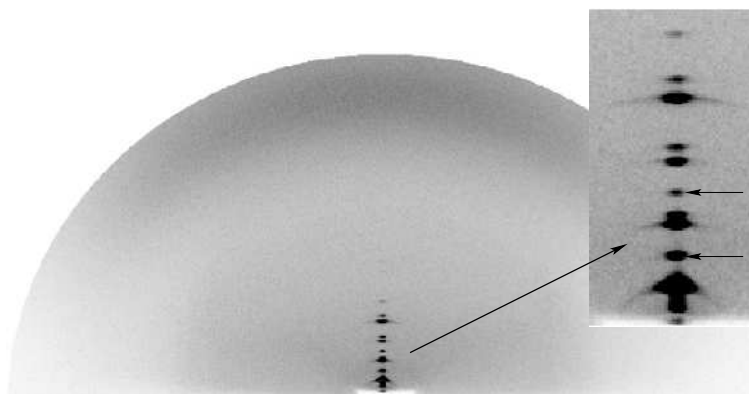


Figure 6.7: Diffraction pattern showing the coexistence of the l_o and l_d phases obtained from an equimolar mixture of sphingomyelin, DOPC and cholesterol at 5°C. Inset shows the small angle region of diffraction pattern on an expanded scale. Two additional reflections (indicated by arrows) of d-spacing 39.5 and 24.0 Å do not fit into either of the lamellar structures. We do not know the origin of these reflections at present.

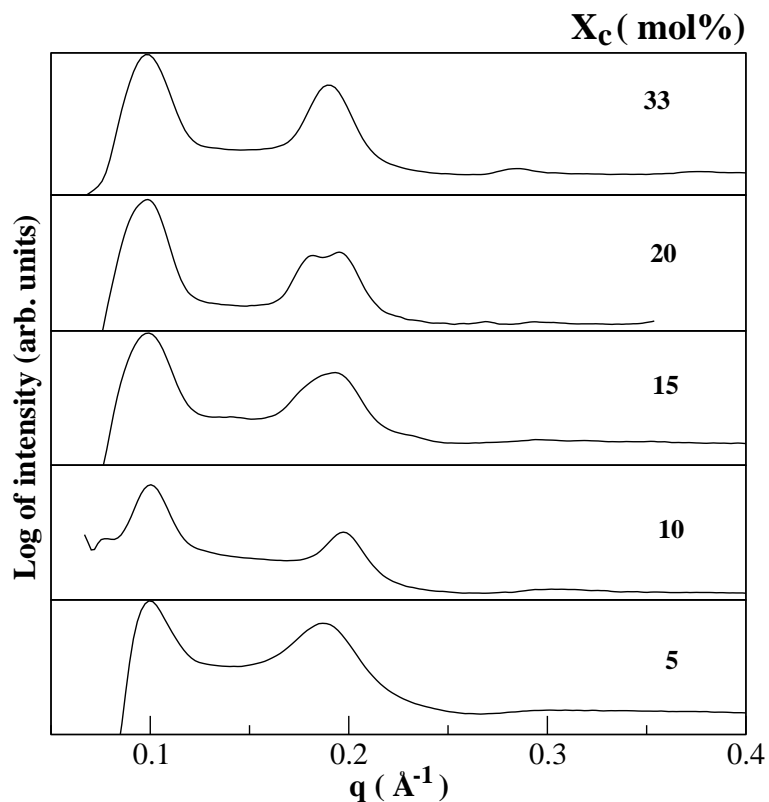


Figure 6.8: Intensity profiles of the small angle region of the diffraction patterns obtained from unoriented samples of ternary raft mixtures in excess water.

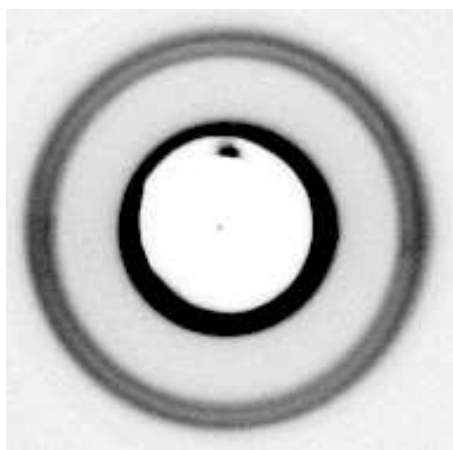


Figure 6.9: Small angle region of the diffraction pattern from an equimolar mixture of DPPC, DOPC at $X_c = 20$ mol% in excess water, showing the coexistence of the l_o ($d = 68.7 \text{ \AA}$) and l_d ($d = 64.8 \text{ \AA}$) phases.

Table 6.2: Lamellar spacings d (Å) obtained from unoriented samples of an equimolar mixture of DPPC and DOPC at various X_c in excess water at $T = 25^\circ\text{C}$. Two sets of spacings correspond to the coexistence of the l_d and l_o phases. The error in d is ± 0.7 Å.

X_c (mol%)	0	2.5	5	10	15	20	33
d	65.9	64.6	67.3	63.7	65.6 ; 68.2	64.1 ; 69.3	66.4

Unoriented samples of the ternary raft mixtures were studied in order to obtain phase behaviour of these mixtures in excess water. Intensity profiles obtained from the small angle region of the diffraction patterns are shown in Fig. 6.8. As mentioned above, the wide angle reflections in the fluid phase were not seen in aligned sample geometry. However, these reflections were easily seen in the case of unoriented samples. This could be due to the much higher amount of the sample in the beam. For $5 \leq X_c < 15$, small angle region of the $I(q)$ vs. q profiles do not show any indication of the second set of lamellar reflections. However, we can easily identify two sets of lamellar reflections at $X_c = 15$ and 20 mol%. Fig. 6.9 shows a diffraction pattern, indicating the coexistence of these two fluid phases. At $X_c = 33$ mol%, we have observed only one fluid phase. The lamellar d-spacings from these ternary mixtures do not change significantly as temperature is increased from 25 to 80°C . A profile of the wide angle reflection from an equimolar ternary raft mixture is shown in Fig. 6.10. The wide angle peak at 4.6 Å seen in these ternary mixtures is comparable to that in the L_α phase of binary mixtures of cholesterol with DPPC. Similar behaviour was obtained from an equimolar ternary mixture of sphigomyelin, DOPC and cholesterol in excess water. These results are consistent with those obtained from the earlier study by Gandhavadi et al. [9]. The lamellar d-spacings obtained from these mixtures are given in table 6.2.

6.4 Discussion

Our experimental results on oriented samples of ternary raft mixtures are summarized in the pseudo binary phase diagram deduced from diffraction data (Fig. 6.4). Aligned multilayers of ternary raft mixtures allow us to detect fluid–fluid coexistence which has not been found

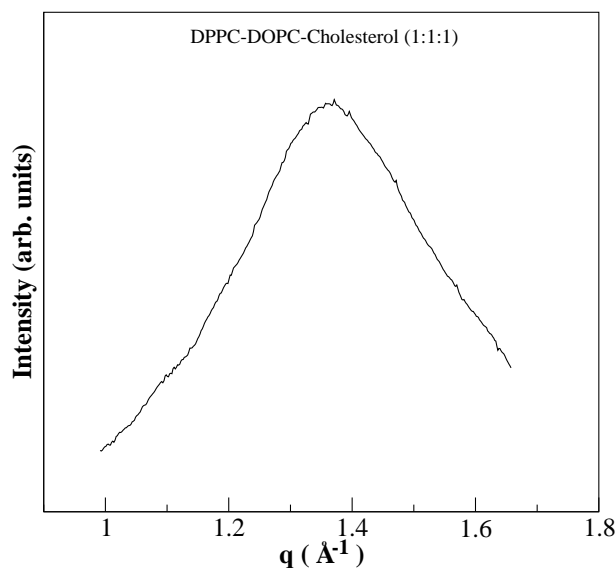


Figure 6.10: Wide angle profile from an unoriented sample of an equimolar mixture of DPPC, DOPC and cholesterol at 25°C in excess water ($d = 4.6 \text{ \AA}$).

in earlier diffraction studies [9]. It is obvious that an equimolar mixture of DPPC and DOPC shows fluid–gel phase separation due to the large difference in the T_m of the two lipids. Therefore, these two phases must be the DPPC–rich $L_{\beta'}$ and DOPC–rich L_{α} phases. This conclusion is supported by the fact that their d-spacings are comparable to those of the pure lipids. As discussed in chapter 3, the presence cholesterol at $X_c > \sim 20$ abolishes the main transition of DPPC, resulting in a fluid liquid ordered (l_o) phase. On the other hand, DOPC membranes remain in the L_{α} phase in the presence of cholesterol, as discussed in chapter 5. Therefore, the two fluid phases coexisting in ternary raft mixtures can be unambiguously identified as l_o , which is rich in DPPC and DOPC–rich l_d phase.

Although we have not explored the entire ternary phase diagram, the partial phase diagram presented here is in good agreement with earlier observations [12, 13, 15]. The ternary phase diagrams obtained from earlier studies using fluorescence microscopy and fluorescence spectroscopy are shown in Fig. 6.11 [14, 15]. A three–phase region similar to that shown in Fig. 6.11 b is also detected in the present study. However, instead of l_o phase, we find a cholesterol induced P_{β} phase to coexist with the gel and l_d phases. This is consistent with the observation of P_{β} phase in binary mixtures of cholesterol with DPPC, as described in chapter 3. The common feature seen in both the phase diagrams (Fig. 6.11 a and b) is

the coexistence of two fluid phases. The closed boundary of the two fluid phase region in Fig. 6.11 a suggests that there is no fluid–fluid coexistence in any of the binary mixtures. This result is consistent with our observations on binary mixtures of cholesterol with DOPC and DPPC. However, in Fig. 6.11 b, the coexistence of the l_o and l_d phases extends upto the cholesterol–POPC axis, indicating $l_o - l_d$ coexistence even in binary mixtures of cholesterol with POPC. Our results on binary mixtures of cholesterol with DOPC do not exhibit such a coexistence. We would expect the phase behaviour of binary mixtures of cholesterol with DOPC and POPC to be similar. Therefore, this discrepancy might be due to the difference in the experimental techniques used to derive these phase diagrams. This situation is reminiscent of that discussed in chapter 3, where different phase behaviour of DPPC–cholesterol mixtures were obtained from spectroscopy studies and from other techniques, such as fluorescence microscopy and x-ray diffraction.

The coexistence of the l_o and l_d phases observed in the present study has been seen in fluorescence microscopy on giant unilamellar vesicles (GUVs) composed of ternary raft mixtures, as shown in the phase diagram (Fig. 6.11 a). These GUVs show uniform fluorescence intensity at high temperatures, indicating a single fluid phase, and a fluid - fluid immiscibility transition at around 25 to 30°C [29]. The present x-ray diffraction study on multilamellar stacks of ternary raft mixtures also shows a transition at around 30°C, below which two fluid phases are found to coexist. Thus our results are consistent with the observations on GUVs discussed above [12, 13, 29]. However, differential scanning calorimetry (DSC) does not show any transition over the temperature range from 3 to 75°C in these mixtures [9]. This could be due to the extremely small enthalpy changes accompanying this transition. As can be seen from Fig. 6.6, d-spacings of both the fluid phases change gradually with temperature and they meet at a higher temperature. However, the change in d-spacing in the l_d phase is not very significant, as found in binary DOPC–cholesterol mixtures. The appearance of a single fluid phase above the miscibility transition temperature indicates that the region of fluid–fluid coexistence in the composition plane shrinks as the temperature is increased [30].

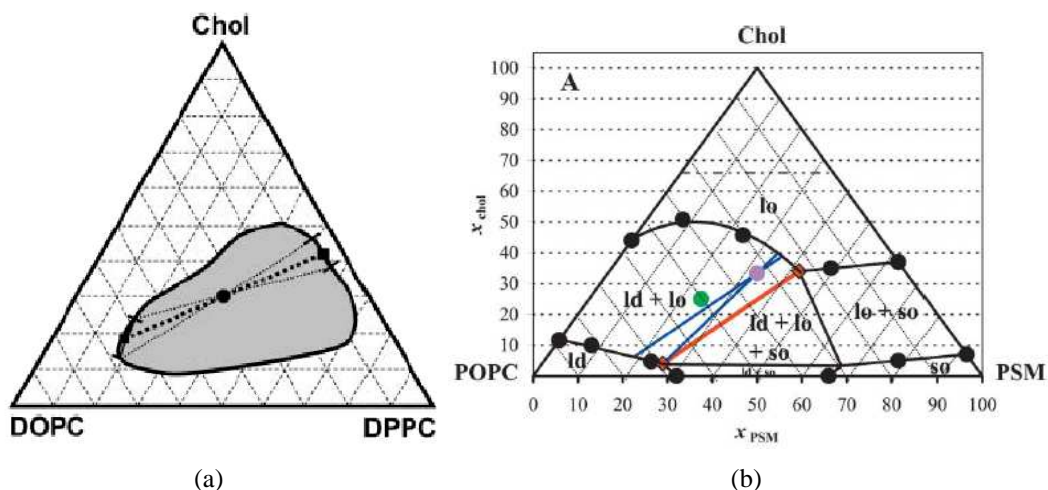


Figure 6.11: Phase diagrams of ternary raft mixtures obtained from fluorescence microscopy at $T = 25^\circ\text{C}$ (a) [14] and fluorescence spectroscopy at $T = 23^\circ\text{C}$ (b) [15]. Thick dashed lines in (a) indicates tie line for 1:1:1 composition. The red tie line in (b) describes the $l_o - l_d$ composition. Blue lines are the tie lines for 1:1:1 composition.

It is somewhat surprising that there was no evidence of $l_o - l_d$ phase separation in earlier diffraction experiments [9]. All previous diffraction studies have mainly been carried out on unoriented samples of equimolar ternary raft mixtures (dispersion of multilamellar vesicles in an excess aqueous environment). As can be seen from Fig. 6.8, there is no indication of coexistence of two phases from an equimolar ternary raft mixture which is consistent with earlier observations [9]. In unoriented samples, we have observed 2-3 lamellar reflections in the fluid phase. As can be seen in Fig. 6.9, the difference of 4-5 Å of the two sets lamellar spacing is just resolved in the 2nd order reflection. Therefore, if the difference in the spacings corresponding to two individual phases is small, it is difficult to resolve them in the small angle region. As shown in Fig. 6.5, the d-spacings of these two phases are comparable at higher X_c . Therefore, we would expect the overlapping of the lamellar spacings of the l_o and l_d phases. Further, it is also not possible to distinguish these phases from their wide angle reflections as the position of the wide angle reflections (~ 4.5 Å) from individual fluid phases coincide (Fig. 6.10). However, at $X_c = 15$ and 20 mol%, we could just detect two lamellar reflections, corresponding to the l_o and l_d phases, as shown in Figs. 6.9 and 6.8, since at lower values of X_c the difference in the d-spacings of these two phases increases, as shown

Table 6.3: The observed magnitude of structure factors $F(h) = \sqrt{\frac{I(h)}{I(h=1)}} \times 100$ calculated from the diffraction data at $X_c = 20$ mol% as a function of temperatures and at $T = 10^\circ\text{C}$ as a function of X_c for the l_o and l_d phases.

$X_c = 20$ mol%	T ($^\circ\text{C}$)	F(1)	F(2)	F(3)	F(4)
l_o	30	10	5.87	2.35	7.06
	25	10	7.06	2.66	8.18
	20	10	7.31	2.92	8.52
	15	10	6.82	2.71	8.94
	10	10	5.8	2.1	8.7
	5	10	5.84	2.4	9.21
l_d	30	10	4.87	4.48	4.5
	25	10	5.24	4.91	3.88
	20	10	5.25	4.87	3.77
	15	10	4.75	4.89	4.1
	10	10	3.36	3.57	3.36
	5	10	3.78	4.59	4.41
$T = 10^\circ\text{C}$		X_c			
l_o	15	10	5.2	2.05	5.8
	20	10	6.4	2.6	9.3
	25	10	5.6	1.8	5.89
l_d	0	10	5.2	5.5	3.7
	15	10	3.97	4.08	3.34
	20	10	4.4	4.8	4.6
	25	10	5.03	4.41	4.3
Phases of reflections		-	-	+	-

in Figs. 6.2 and 6.5. It can be seen from the phase diagram (Fig. 6.4) that the equimolar ternary mixture is situated very close to the phase boundary between the two-phase region and the l_o phase. Therefore, small compositional error can easily take the system away from the two-phase region. The difference in the d-spacings of the two phases decreases with increasing X_c , suggesting that cholesterol affects both the phases significantly.

There is some controversy in the literature regarding the cholesterol content of the l_o and l_d phases. It is believed that the l_o phase is rich in cholesterol, whereas the l_d phase contains much less cholesterol. However, a recent NMR study on the ternary raft mixtures suggests that the cholesterol contents in these two phases are similar [14]. In contrast, the tie lines obtained in ref. [15] clearly indicate that cholesterol content in the l_o phase is very different

from that in the l_d phase. This is due to the fact that the binary system POPC–cholesterol itself shows a l_o – l_d coexistence, according to the experimental technique employed in ref. [15]. On the other hand, the tie lines presented in ref. [14] make a much smaller angle with the DPPC–DOPC axis at all X_c for which l_o and l_d phases were detected. In this situation, both phases have similar cholesterol content, although the amount of the two phases depends on the composition of the ternary mixtures.

It is interesting to note that diffraction peaks corresponding to the l_o and l_d phases were well resolved at $X_c < 33$ mol%. However, these peaks gradually get closer as X_c is increased from 15 mol% (Fig. 6.2), and the two d-spacings become comparable (Fig. 6.5). The lamellar d-spacing of the l_o phase decreases, whereas it increases slightly in the l_d phase with increasing X_c . This is consistent with the fact that the d-spacing does not change much with increasing X_c in binary DOPC–cholesterol mixtures, whereas it decreases significantly as X_c is increased in binary DPPC–cholesterol mixtures. It is evident from Fig. 6.5 that there exists a threshold value of X_c , above which the d-spacings of both the phases merge. The threshold value of X_c decreases as the temperature is increased. It is possible that there is a critical point at which the fluid–fluid immiscibility transition is continuous. Presently we cannot determine the critical point as we have studied only one slice of the ternary phase diagram. These results suggest that both phases contain a considerable amount of cholesterol. If we assume that all the cholesterol gets into the l_o phase then we would expect the fluid–fluid coexistence to be seen for all X_c . The fact that at $X_c > 35$ mol%, the d-spacing of both the l_o and l_d phases become comparable, leading to a single lamellar d-spacing, rules out this possibility. This is also supported by the fact that GUVs show uniform fluorescence intensity at $X_c > 40$ mol% [13]. Therefore, a single lamellar spacing in the diffraction experiment (Fig. 6.2 f) and uniform fluorescence intensity on GUVs at higher X_c show that the phase coexistence disappears at these values of X_c .

In order to understand the partitioning of cholesterol into these two fluid phases, we have examined binary mixtures of cholesterol with DPPC and DOPC, which have already been discussed in detail in chapters 3 and 5, respectively. Our aim was to compare the l_o

and l_d phases obtained from ternary raft mixtures with the corresponding binary mixtures. As discussed in chapter 5, the d-spacings of DOPC–cholesterol mixtures do not seem to change with cholesterol content and the electron density profiles obtained at all X_c look similar. The electron density of the broad trough region due to the terminal methyl groups does not increase significantly in the presence of cholesterol. However, in DPPC–cholesterol mixtures, the secondary maxima is clearly seen due to an increase in the electron density in the presence of cholesterol. In order to compare these features, it is necessary to construct the electron density profiles of the l_o and l_d phases from ternary raft mixtures. Transbilayer electron density profiles were constructed from the diffraction data presented in table 6.3. Electron density profiles obtained from the diffraction data at different X_c are shown in Figs. 6.12 and 6.13. Only one combination of phases (- - + -) of the reflections gives a realistic electron density profile, as discussed in chapter 5. This combination of phases is the same as that found in DOPC–cholesterol mixtures, and it does not alter with either X_c or temperature. The variation in relative intensities of different reflections of the l_o and l_d phases of ternary raft mixtures with X_c is similar to that found in binary mixtures of cholesterol with DPPC and DOPC, respectively. The electron density profiles of the l_d and l_o phases obtained at different X_c and temperature in ternary raft mixtures is very similar to those found in binary mixtures of cholesterol with DOPC and DPPC at similar X_c , respectively. The broad trough in the electron density profiles of the l_d phase due to the terminal methyl groups gets narrower as X_c is increased, consistent with the results obtained in binary DOPC–cholesterol mixtures. As discussed in chapter 5, the electron density profiles at a given X_c do not show any significant change with increasing temperature. A similar trend has been observed in the l_d phase of ternary raft mixtures, as shown in Fig. 6.14. The electron density profiles of the l_o phase (Fig. 6.13) show a secondary maxima at $\pm 10 \text{ \AA}$ due to the presence of cholesterol as found in DPPC–cholesterol mixtures, and in agreement with earlier studies [9, 27]. These profiles also do not show any considerable change with temperature (Fig. 6.15). Bilayer thickness of the l_o and l_d phases derived from the electron density profiles (Figs. 6.15 and 6.14) are found to be 47.5 \AA and 40 \AA , respectively, which are in good agreement with those obtained

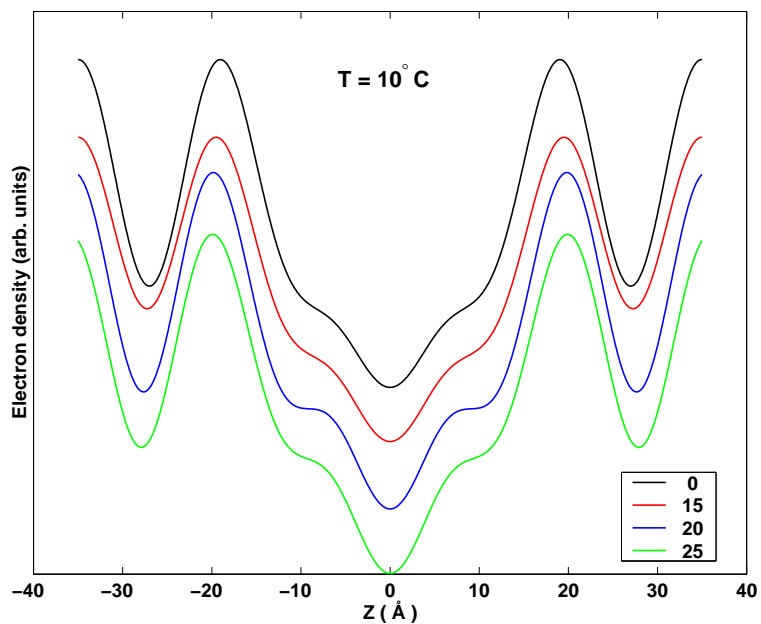


Figure 6.12: Transbilayer electron density profiles of the l_d phase of an equimolar mixture of DPPC and DOPC as a function of X_c at $T = 10^\circ\text{C}$ (data are given in table 6.3).

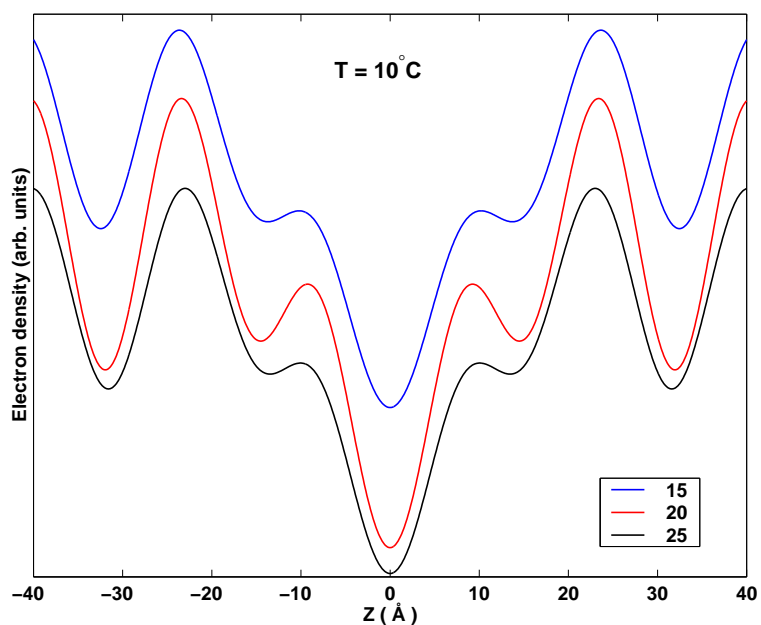


Figure 6.13: Transbilayer electron density profiles of the l_o phase of an equimolar mixture of DPPC and DOPC as a function of X_c at $T = 10^\circ\text{C}$, calculated from the data given in table 6.3.

in an earlier study [9].

Although electron density profiles, relative intensities of reflections and d-spacings obtained in the l_o and l_d phases resemble those obtained from binary mixtures of cholesterol with DPPC and DOPC, respectively, these results are not sufficient to quantify precisely the cholesterol contents of these phases. As the electron density of the head group and the terminal methyl group gets modified in the presence of cholesterol, it is difficult to estimate the cholesterol composition just by subtracting from these profiles those obtained from the pure system. However, comparing the phase behaviour of DPPC–cholesterol mixtures, discussed in chapter 3, we can actually put a lower limit on the cholesterol content of the l_d phase assuming that all the DPPC gets into the l_o phase and all DOPC is in the l_d phase. For example, the l_o - P_β boundary in binary mixtures of DPPC–cholesterol occurs at $X_c = 22$ mol% at 10°C , whereas, it is detected at $X_c = 15$ in ternary mixtures at the same temperature. Therefore, cholesterol concentration in the ternary mixtures is about 26 mol% with respect to DPPC. If DPPC needs maximum 22% cholesterol to exhibit the P_β phase, then the rest ~ 5 mol% cholesterol must go into the DOPC bilayers. Similarly, at $X_c = 10$ mol%, the ternary mixture behaves like a 12.5 mol% mixture of cholesterol in DPPC and the $L_{\beta'}$ – P_β boundary was detected in both the systems. In this case cholesterol content with respect to DPPC in the ternary mixtures is ~ 18 mol%. Therefore, again $\sim 5\%$ cholesterol can be present in DOPC bilayers. For $15 < X_c < 35$, there is no P_β phase in ternary mixtures. At these X_c , any amount of cholesterol > 22 mol% can be accommodated in DPPC and the rest can be incorporated in DOPC. Our results indicate that at lower X_c ($< 15\%$), cholesterol content in both the phases are very different, whereas at higher X_c (> 25), partitioning of cholesterol into the l_o and l_d phases cannot be determined conclusively. These results suggest that cholesterol has a greater affinity for DPPC at low concentrations. However, at higher X_c , we cannot comment on the preferential affinity of cholesterol for the lipids from the present study. As discussed in chapter 5, cholesterol has a rigid moiety and a small hydrophilic head (-OH). On the other hand, DOPC has a *cis* double bond, resulting in a kink in the chain. Therefore, cholesterol molecules can pack efficiently in DPPC bilayers compared to DOPC, as the kink in DOPC

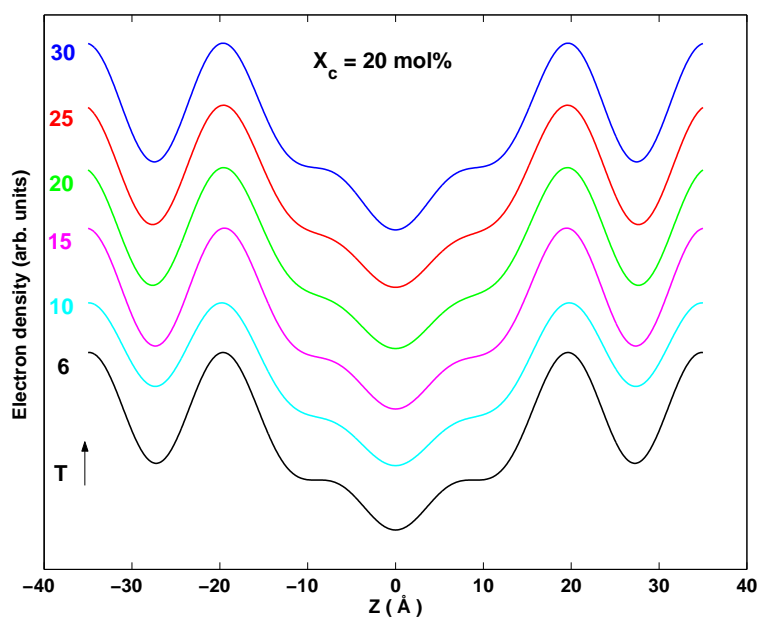


Figure 6.14: Electron density profiles of the l_d phase obtained from an equimolar mixture of DPPC and DOPC at $X_c = 20 \text{ mol\%}$ as a function of temperature indicated by the labels with the profiles (data are given in table 6.3).

can hinder efficient packing of cholesterol [27]. As discussed in chapter 5, the stretching of the unsaturated chains of DOPC is not as effective as in the case of DPPC membranes in the presence of cholesterol, resulting in the broad trough in the electron density profile at the center of the bilayer, as shown in Figs. 6.12 and 6.14.

As discussed above, a phase separation occurs even in the absence of cholesterol in binary DPPC–DOPC mixtures below T_m . However, these are the $L_{\beta'}$ and L_{α} phases. The fact that binary DPPC–cholesterol mixtures exhibit the l_o phase at higher X_c and the ternary raft mixtures show coexistence of l_o and l_d at similar X_c implies that gel phase gets replaced by the l_o phase in the presence of cholesterol. Therefore, it is conceivable that cholesterol is not essential for phase separation in ternary mixtures as proposed by Milhiet et al. [31]. Function of cholesterol, in these model system is to transform the gel phase into the l_o phase. On the other hand, studies on the influence of sterol structure on membrane lipid domains in binary mixtures by Xu et al. suggest that cholesterol can induce lipid domain formation [32].

The coexistence of the two fluid phases similar to that seen in ternary mixtures below T_m has also been found in binary lipid–cholesterol mixtures using spectroscopy techniques,

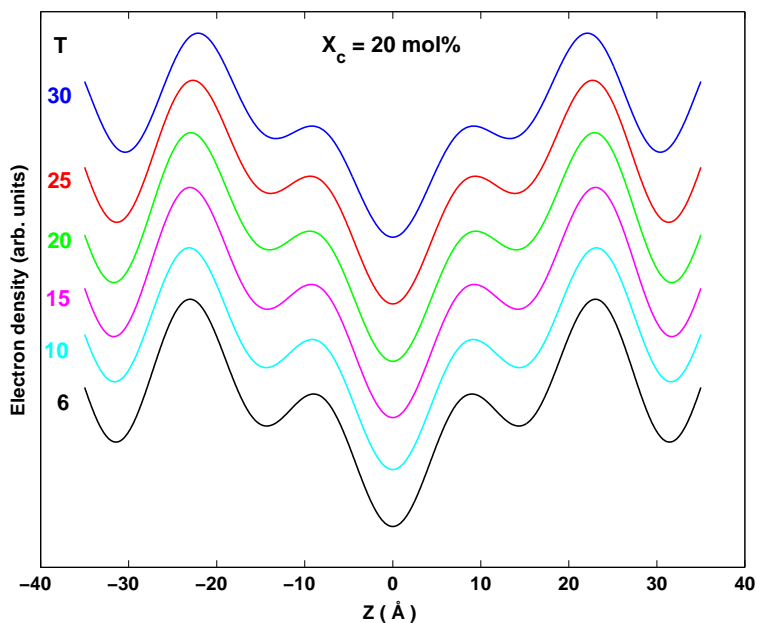


Figure 6.15: Electron density profiles of the l_o phase obtained from an equimolar mixture of DPPC and DOPC at $X_c = 20$ mol% as a function of temperature indicated by the labels with the profiles (data are given in table 6.3).

such as NMR [26]. However, the fluid–fluid immiscibility occurs in binary mixtures above T_m , whereas it occurs below T_m in ternary mixtures. None of the earlier diffraction studies of binary lipid–cholesterol mixtures have reported such a coexistence above T_m . Therefore, the coexistence of the two fluid phases seen in spectroscopy study of binary mixtures above T_m could be due to the presence of microscopic domains of different chain conformational order of the lipids from the rest of the membranes. However, the coexistence in ternary mixtures seen below T_m is actually a macroscopic phase separation, as it is seen by present diffraction study and by fluorescence microscopy on GUVs.

6.5 Conclusion

We have observed for the first time a fluid–fluid phase separation in ternary mixtures of DPPC, DOPC and cholesterol using diffraction techniques. Similar behaviour was also found in the case of sphigomyelin–DOPC–cholesterol mixture. We have compared the electron density profiles of the l_o and l_d phases in ternary mixtures with their respective binary mixtures in order to estimate the cholesterol contents of both the fluid phases. In the present study

we have not been able to quantify the cholesterol content of each phase at $X_c > 20$. However, at low X_c (<15) we have estimated the cholesterol content of these phases by comparing the phase boundaries in the ternary mixtures with those in the binary DPPC–cholesterol mixtures. Further studies are required to precisely determine the partitioning of cholesterol into the two coexisting fluid phases.

Bibliography

- [1] M. Edidin, *Annu. Rev. Biophys. Biomol. Struct.* **32**, 257 (2003).
- [2] R. Lipowsky, *J. Biol. Phys.* **28**, 195 (2002).
- [3] K. Simons and E. Ikonen, *Nature* **387**, 569 (1997).
- [4] K. Gaus, E. Gratton, E. P. W. Kable, A. S. Jones, I. Gelissen, and L. Kritharides, *Proc. Natl. Acad. Sci. U.S.A.* **100**, 15554 (2003).
- [5] T. P. W. McMullen, R. N. A. H. Lewis, and R. N. McElhaney, *Curr. Opin. colloid Interface Sci.* **8**, 459 (2004).
- [6] D. A. Brown and E. London, *J. Biol. Chem.* **275**, 17221 (2000).
- [7] E. London and D. A. Brown, *Biochim. Biophys. Acta* **1508**, 182 (2000).
- [8] T. J. McIntosh, A. Vidal, and S. A. Simon, *Biophys. J.* **85**, 1656 (2003).
- [9] M. Gandhavadi, D. Allende, A. Vidal, S. A. Simon, and T. J. McIntosh, *Biophys. J.* **82**, 1469 (2002).
- [10] L. Finegold, ed. *Cholesterol in Membrane Models* (CRC Press, Boca Raton, FL, 1993).
- [11] H. Heerklotz, *Biophys. J.* **83**, 2693 (2002).
- [12] S. L. Veatch and S. L. Keller, *Phys. Rev. Lett.* **89**, 268101 (2002).
- [13] S. L. Veatch and S. L. Keller, *Biophys. J.* **85**, 3074 (2003).
- [14] S. L. Veatch, I. V. Polozov, K. Gawrisch, and S. L. Keller, *Biophys. J.* **86**, 2910 (2003).

- [15] R. F. M. de Almeida, A. Fedorov, and M. Prieto, *Biophys. J.* **85**, 2406 (2003).
- [16] D. Scherfeld, N. Kahya, and P. Schwille, *Biophys. J.* **85**, 3758 (2003).
- [17] G. W. Feigenson and J. T. Buboltz, *Biophys. J.* **80**, 2775 (2001).
- [18] H. M. McConnell and M. Vrljic, *Annu. Rev. Biophys. Biomol. Struct.* **32**, 469 (2003).
- [19] H. M. McConnell and A. Radhakrishnan, *Biochim. Biophys. Acta* **1610**, 159 (2003).
- [20] T. Baumgart, S. T. Hess, and W. W. Webb, *Nature* **425**, 821 (2003).
- [21] H. A. Rinia, M. M. E. Snel, J. P. J. M. van der Eerden, and B. de Kruijff, *FEBS Lett.* **501**, 92 (2001).
- [22] J. Korlach, P. Schwille, W. W. Webb, and G. W. Feigenson, *Proc. Natl. Acad. Sci. U.S.A.* **96**, 8461, (1999).
- [23] M. Ge, K. A. Field, R. Aneja, D. Holowka, B. Baird, and J. H. Freed, *Biophys. J.* **77**, 925 (1999).
- [24] P. E. Milhiet, C. Domec, M. Giocondi, N. V. Mau, F. Heitz, and C. Le. Grimellec, *Biophys. J.* **81**, 547 (2001).
- [25] N. Kahya, D. Scherfeld, K. Bacia, B. Poolman, and P. Schwille, *J. Biol. Chem.* **278**, 28109 (2003).
- [26] M. R. Vist and J. H. Davis, *Biochemistry* **29**, 451 (1990).
- [27] T. J. McIntosh, *Biochim. Biophys. Acta* **513**, 43 (1978).
- [28] W. Knoll, G. Schmidt, K. Ibel, and E. Sackmann, *Biochemistry* **24**, 5240 (1985).
- [29] C. Dietrich, L. A. Bagatolli, Z. N. Volovyk, N. L. Thompson, M. Levi, K. Jacobson, and E. Gratton, *Biophys. J.* **80**, 1417 (2001).
- [30] S. L. Veatch and S. L. Keller, *Phys. Rev. Lett.* **94**, 148101 (2005).

[31] P. E. Milhiet, M. Giocondi, and C. Le. Grimellec, *J. Biol. chem.* **277**, 875 (2002).

[32] X. Xu and E. London, *Biochemistry* **39**, 843 (2000).